

Role of GABA_A-mediated inhibition in controlling the responses of regular spiking cells in turtle visual cortex

JAIME G. MANCILLA AND PHILIP S. ULINSKI

Committee on Neurobiology and Department of Organismal Biology and Anatomy, University of Chicago, Chicago

(RECEIVED June 22, 1999; ACCEPTED August 10, 2000)

Abstract

The visual cortex of freshwater turtles contains pyramidal cells, which have a regular spiking (RS) firing pattern, and several categories of aspiny, inhibitory interneurons. The interneurons show diverse firing patterns, including the fast spiking (FS) pattern. Postsynaptic potentials (PSPs) evoked in FS cells by visual stimulation of the retina reach their peak amplitudes as much as 200 ms before PSPs in RS cells (Mancilla et al., 1998). FS cells could, consequently, control the amplitudes of light-evoked PSPs in RS cells by producing disynaptic, feedforward inhibitory postsynaptic potentials (IPSPs) that overlap in time with geniculocortical excitatory postsynaptic potentials (EPSPs). Since FS cells receive recurrent, excitatory inputs from RS cells, they could also control the amplitudes of light-evoked PSPs in RS cells via polysynaptic, feedback inhibition. The *in vitro* geniculocortical preparation of *Pseudemys scripta* was used to characterize the temporal relationships of EPSPs and IPSPs produced in RS cells by electrical activation of geniculate afferents and by diffuse light flashes presented to the retina. GABA_A receptor-mediated inhibition was blocked using extracellular application of bicuculline (3.5 μM) or intracellular perfusion of picrotoxin (1 mM) in individual RS cells. Electrical stimulation of thalamic afferents produced compound PSPs. Blockade of GABA_A receptor-mediated IPSPs with either bicuculline or picrotoxin provided evidence for both early and late IPSPs in RS cells. Analysis of the apparent reversal potentials of light-evoked PSPs indicated the existence of early IPSPs during the first 140–300 ms following light onset. Light responses of cells perfused with picrotoxin diverged from control light responses at about 300 ms after light onset and had maximum amplitudes that were significantly different from control light responses. These experiments indicate that the responses of RS cells to both electrical and natural stimulation of geniculate afferents are controlled by both early and late IPSPs, consistent with activation of both feedforward and feedback pathways.

Keywords: Neocortex, Pyramidal cells, Interneurons, Excitatory postsynaptic potentials, Inhibitory postsynaptic potentials

Introduction

Neurons within the sensory cortices of vertebrates form microcircuits of interconnected neurons (Davis & Sterling, 1979; Gilbert, 1983; Connors & Kriegstein, 1986; Kriegstein & Connors, 1986; Douglas & Martin, 1991). The principal input to these circuits are thalamic afferents that synapse on excitatory cells with spiny dendrites. These inputs are excitatory and generate excitatory postsynaptic potentials (EPSPs) in spiny cells. In mammals, the spiny cells are stellate cells of layer IV and pyramidal cells in several layers. In turtles, they are principally layer 2 pyramidal cells. Spiny cells in both mammals and turtles generate a regular spiking (RS) train of action potentials that show spike-frequency adaptation following intracellular current injection (McCormick et al., 1985; Chagnac-Amitai & Connors, 1989; Connors et al., 1982; Connors

& Gutnick, 1990; Franceschetti et al., 1995; Chen et al., 1996; Gray & McCormick, 1996). Thalamic afferents also effect excitatory synapses on inhibitory, aspiny neurons (Garey & Powell, 1971; Ebner & Colonnier, 1975; Peters et al., 1976; Smith et al., 1980; Peters & Fairén, 1978; Anderson et al., 1994). Aspiny cells show a variety of firing patterns (e.g. Azouz et al., 1997; Cauli et al., 1997; Kawaguchi & Kubota, 1997; Gupta et al., 2000), but frequently show a fast spiking (FS) pattern with little spike-frequency adaptation (McCormick et al., 1985; Chagnac-Amitai & Connors, 1989; Connors & Gutnick, 1990; Kawaguchi, 1993, 1995; Chen et al., 1996; Gray & McCormick, 1996; Thomson et al., 1996). They make inhibitory synapses on spiny cells and receive excitatory synapses from the recurrent collaterals of spiny cells. The output from the circuits is formed by the axons of pyramidal cells in both mammals and turtles.

The structure of cortical microcircuits implies that RS cells are potentially subjected to two forms of inhibitory control. They receive disynaptic inhibitory postsynaptic potentials (IPSPs) via feedforward inhibition, and polysynaptic IPSPs via feedback inhibition

Address correspondence and reprint requests to: Philip S. Ulinski, Department of Organismal Biology and Anatomy, University of Chicago, 1027 E. 57th Street, Chicago, IL 60637, USA.

mediated by the recurrent collaterals of spiny cells. An understanding of how feedforward and feedback inhibition regulate the discharge of spiny cells depends upon a knowledge of the relative timing of thalamocortical EPSPs in spiny cells and the IPSPs generated *via* feedforward and feedback mechanisms. The classic work on the timing of EPSPs and IPSPs in cortical circuits was based on studies using electrical activation of thalamic afferents (Li et al., 1960; Anderson, 1965; Watanabe et al., 1966; Eccles, 1969; Ferster & Lindström, 1983). These studies reported that activation of thalamic afferents results in EPSP-IPSP sequences in spiny cells, with the relative timing of the IPSP determined by an additional synaptic delay in the disynaptic pathway. However, Mancilla et al. (1998) found that postsynaptic potentials (PSPs) evoked in FS cells by visual stimulation of the retina in turtles reach their peak amplitudes as much as 200 ms before those in RS cells. FS cells could, consequently, control the amplitudes of light-evoked PSPs in RS cells by producing IPSPs that overlap in time with geniculocortical excitatory postsynaptic potentials (EPSPs), as well as through feedback inhibition.

The *in vitro* geniculocortical preparation of the turtle, *Pseudemys scripta*, was used in this study to characterize the temporal relationships of thalamocortical EPSPs and GABA_A receptor-mediated IPSPs in RS cells. This was done by studying the voltage dependence of PSPs evoked by both electrical activation of geniculate afferents and stimulation of the retina with diffuse light flashes. GABA_A receptor-mediated inhibition was blocked using extracellular application of bicuculline or intracellular perfusion of picrotoxin. The experiments indicate that the firing of RS cells is controlled by GABA_A receptor-mediated inhibition *via* both feedforward and feedback pathways.

Materials and methods

Tissue preparation

Freshwater turtles of the genus *Pseudemys* were anesthetized by intraperitoneal injections of sodium Brevital (50 mg/kg) and cool-

ing until torpid, or by sodium Brevital injections without cooling. The geniculocortical preparation was obtained by removing the brain caudal to the olfactory bulbs and rostral to the optic tectum, but keeping the eyes attached (Fig. 1). One cortical hemisphere and the contralateral eye were retained for the experiments. Cuts were made rostrocaudally along the medial cortex and mediolaterally at the rostral and caudal ends of the hemisphere to unfold the cortex and expose its ventricular surface. The retina was exposed for direct illumination by removing the anterior part of the eye (Fig. 1A). The preparation for electrical stimulation studies was obtained using the same procedure, except that the optic nerve was cut (Fig. 1B). Preparations were kept at room temperature (20–22°C) and perfused with oxygenated (95% O₂/5% CO₂) turtle Ringer's solution containing (in mM) 96.5 NaCl, 2.6 KCl, 2.0 MgCl₂, 4.0 CaCl₂, 31.5 NaHCO₃, and 10.0 dextrose (Mori et al., 1981). The solution was maintained at a pH of 7.6.

Recording methods

Intracellular sharp electrodes (80–140 MΩ) were made from thick-walled (O.D. 1.2 mm, I.D. 0.60 mm) borosilicate glass and filled with 4.0 M potassium acetate. Pipettes were advanced through the tissue at known angles using a Narashige (Narashige, Tokyo, Japan) hydraulic microdrive positioned on a Newport (Newport, Fountain Valley, CA) motion controller. The position of the microelectrode was obtained by measuring the *X* and *Y* positions on the motion controller and its depth in the tissue calculated by multiplying the depth reading from the microdrive by a correction factor for the angle of the pipette. Experiments were done in current clamp using an Axoclamp 2A preamplifier connected to a Nicolet 410 (Nicolet, Madison, WI) digital oscilloscope. Data were stored on floppy disks for off-line analysis.

Visual and electrical stimulation

A bipolar stimulating electrode placed in the lateral forebrain bundle was used to deliver 100-ms current pulses at 1 Hz for electrical

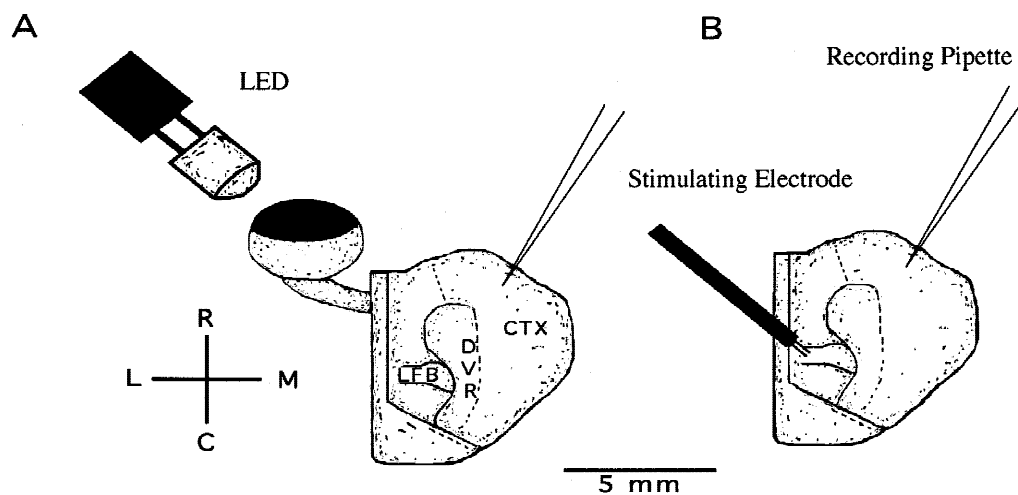


Fig. 1. Genulocortical preparation. A: A preparation with the eye attached was used for light experiments. The location of the dissected dorsal ventricular ridge (DVR), the lateral forebrain bundle (LFB), and the cortex (CTX) are indicated. Rostro-caudal and lateral-medial axes are also indicated. A 640-nm light emitting diode (LED) is positioned 3 mm from the retina to provide the light stimulus while responses of cortical cells are recorded using sharp electrodes. B: A preparation with the eye removed was used for electrical-stimulation experiments. A bipolar stimulating electrode is placed in the LFB to electrically stimulate the thalamocortical axons while responses of cortical cells are recorded using a sharp electrode.

stimulation experiments. Responses were averaged over 20 trials. Stimulus intervals were controlled using a WPI 1830 interval generator module (World Precision Instrument, New Haven, CT) connected to a WPI 1831 pulse train modulator. Stimulus intensity was controlled by using a WPI 305 stimulus isolator adjusted to deliver current at threshold (T) or multiples of the threshold intensity ($\times T$). Threshold intensity varied between cells and was defined as the first intensity producing a PSP that could be distinguished from baseline noise by visual inspection.

The preparation was maintained in the dark for 1 h prior to beginning the experiments using visual stimulation. Square, 640-nm light pulses from a light-emitting diode positioned 3 mm from the retina were used to provide diffuse illumination to the dark-adapted retina. This wavelength is optimal for activating turtle ganglion cells which are dominated by input from red cones. Light pulses varied in intensity from 0 to 2.6×10^4 photons $\mu\text{m}^{-2} \text{s}^{-1}$ and had durations of 1 s. The retina was maintained in the dark for 1.5 min between trials. Response threshold was measured with an accuracy of 2^{-13} photons $\mu\text{m}^{-2} \text{s}^{-1}$. The pulse duration was controlled using the same interval generator module and pulse train used for electrical stimulation. Stimulus intensity was controlled using the same stimulus isolator used for electrical stimulation. Randomly interleaved intensities were used to generate intensity–response (IR) functions.

Drug application

Bath application of bicuculline methiodide (3.5 μM , Sigma, St. Louis, MO) was used to block GABA_A receptor-mediated inhibition in the cortex. Intracellular blockade of GABA_A receptor-mediated inhibition was accomplished by allowing picrotoxin to freely diffuse into cells with sharp pipettes filled with picrotoxin (1 mM, Sigma) in 4 M potassium acetate.

Data analysis

Intracellular records were analyzed using Kaleidagraph (Synergy Software, Reading, MA) to obtain the latency, peak time, and amplitude of each response. To determine the latency, the average of the prestimulus baseline was determined and the time of the first deviation from the baseline was taken as the response onset. The peak time is the time from the onset of the stimulus to the maximum amplitude of the response. The maximum amplitudes of responses without action potentials were the peaks of the depolarizing potentials. When action potentials were present, the amplitudes of the underlying potentials were measured with the action potentials stripped. Amplitudes of responses (R) were plotted as a function of the intensity of the light pulse (I) to produce intensity–response (IR) functions. Data were fit with a Boltzmann equation of the form

$$R = R_{\max} [I + \exp\{-(I - I_{50})/k\}],$$

where R_{\max} is the maximal response, I_{50} is the light intensity at half-maximal response, and k is a slope factor.

Amplitude measurements for reversal-potential analysis were carried out with responses that were subthreshold to action potential generation and were, therefore, uncontaminated by currents due to the voltage-gated conductances involved in spike generation. Measurements were obtained by subtracting the average membrane potential during the 30 ms before stimulus onset from the

membrane potential at the time for which the reversal potential was measured. No measurements were made at stimulus onset and offset because stimulus artifacts were present at these times. Plots of PSP amplitude as a function of holding potential were fit with second-order polynomials to determine apparent reversal potentials for individual cells at each interval for each of the cells. Averages were taken at equivalent time points over several cells and used to plot the mean apparent reversal potential as a function of time. The apparent reversal potential is a weighted mean of the reversal potentials of all of the currents flowing through the membrane of the cell at a given point in time. It equals the resting membrane potential of the cell in the absence of synaptic or voltage-gated currents. Activation of synaptic currents shifts the apparent reversal potential away from the resting membrane potential. Since excitatory synapses in turtle cortical neurons have reversal potentials of approximately 0 mV (Blanton & Kriegstein, 1992), activation of excitatory synapses shifts the apparent reversal potential in the depolarizing direction. Since GABA_A receptor-mediated inhibitory synapses have reversal potentials of approximately -70 mV (Blanton & Kriegstein, 1991), activation of inhibitory synapses shifts the apparent reversal potential in the hyperpolarizing direction. Simultaneous activation of excitatory and inhibitory synapses shifts the apparent reversal potential in either direction, depending on the relative magnitudes of the excitatory and inhibitory synapses. A shift of the apparent reversal potential in the hyperpolarizing direction is, then, a clear indication of the activation of inhibitory synapses. A shift in the depolarizing direction can indicate either activation of only excitatory synapses, or simultaneous activation of excitatory and inhibitory synapses with the magnitude of the excitatory currents being larger than that of the inhibitory currents.

All statistical data are reported as means and standard errors.

Results

Characterization of RS cells

This study is based on 26 cells with biophysical characteristics and depths in the cortex consistent with those of pyramidal cells (see discussion in Mancilla et al., 1998). All cells exhibited spike-frequency adaptation (Fig. 2A) in response to depolarizing current injections, had spike thresholds of -41.1 ± 1.3 mV, spike half-widths of 2.2 ± 0.1 ms, resting membrane potentials of -65.4 ± 1.5 mV, and depths of 192.4 ± 15.4 μm that were generally consistent with RS cells described in earlier studies (Connors & Kriegstein, 1986; Mancilla et al., 1998). Cells had voltage–current plots that showed rectification at negative currents (Fig. 2B). They were distributed throughout the rostrocaudal extent of the cortex.

Electrically evoked PSPs

General features

PSPs evoked by electrical stimulation of thalamic afferents were obtained in six RS cells. Cells were held as close to their resting membrane potentials (-62.6 mV to -75.7 mV) as was possible. PSPs were compound events consisting of an early depolarization followed by a short latency hyperpolarization and a late hyperpolarization lasting approximately 800 ms. The early depolarization varied in size and could be shunted by the IPSP (Fig. 3A, top). PSPs had a mean latency of 22.7 ± 0.6 ms, a mean peak time of 62.9 ± 5.2 ms, and a mean amplitude of 4.5 ± 3.6 mV.

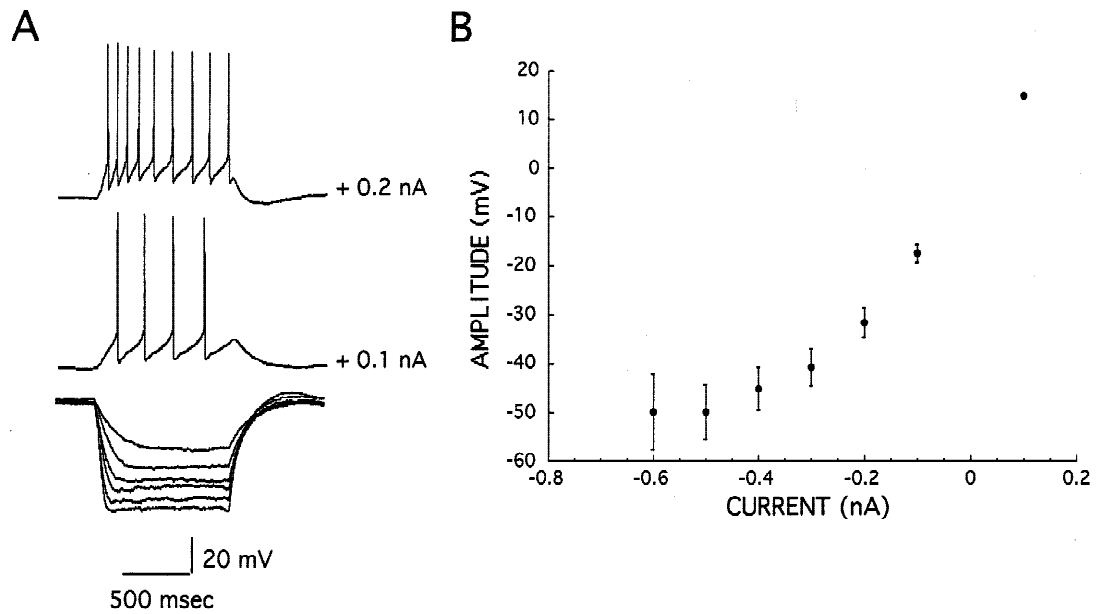


Fig. 2. Biophysical characterization of RS cells. A: Voltage responses to negative current pulses ranging from -0.1 to -0.6 nA are shown below the voltage responses to 0.1 and 0.2 nA current pulses. B: Negative current pulses and positive current pulses that did not produce action potentials were used to create a plot of mean amplitudes of voltage responses at 500 ms as a function of current intensity.

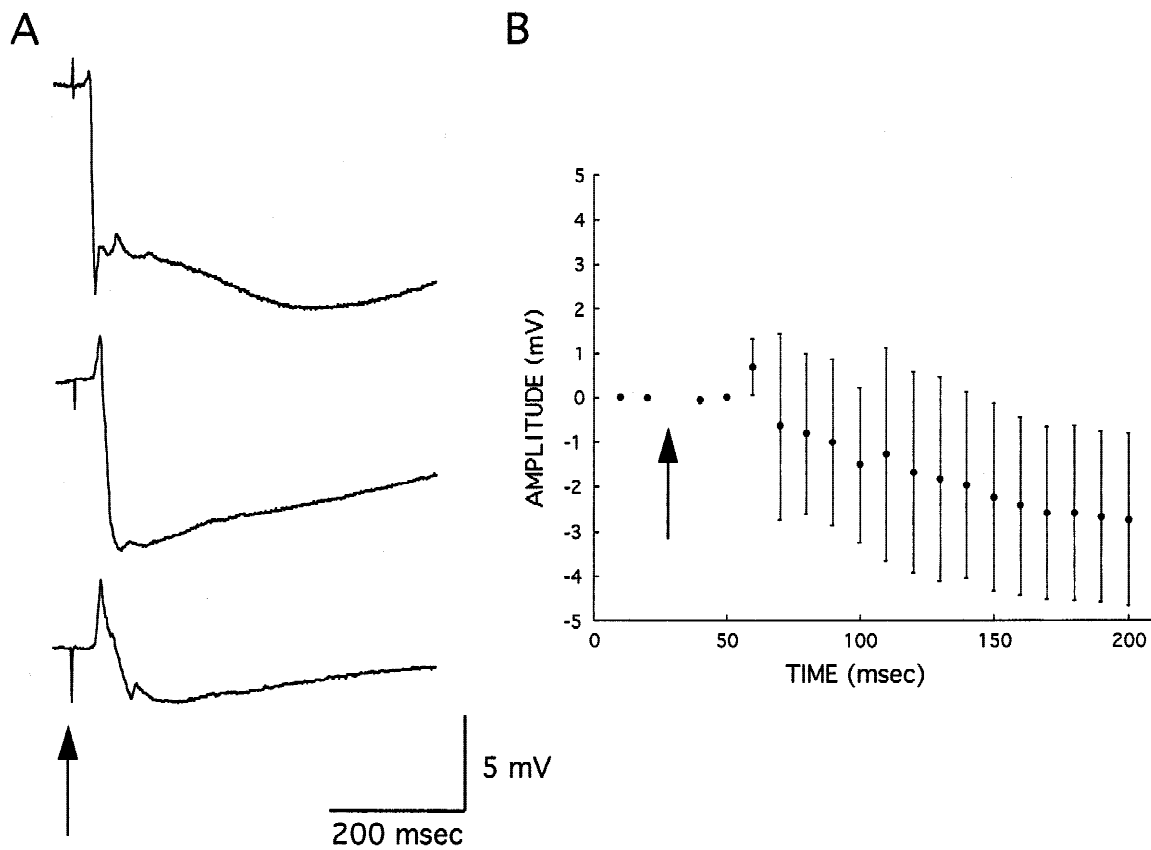


Fig. 3. Electrically evoked PSPs. A: Representative examples of responses of RS cells to electrical stimulation of thalamic afferents obtained at a holding potential of -60 mV. Traces show that the EPSP preceding the IPSP can be significantly reduced by the IPSP (top), can appear as a minor component of the response (middle) or as a major component of the response (bottom). These traces were obtained by averaging 20 responses at 1-s intervals. Stimulation at 30 ms produced an artifact that can be seen in the trace (arrow). B: The mean amplitude of responses of four RS cells to stimulation of the LFB at twice threshold is plotted as a function of time. The amplitude measurements obtained at 30 ms (arrow) were omitted to eliminate the stimulus artifact from the plot.

Four cells were held at -60 mV and stimulated with an intensity of 2T to create a plot of the mean amplitude of the PSPs as a function of time (Fig. 3B). The plot showed an initial depolarization with a peak 30 ms after the stimulus onset, followed by a hyperpolarization lasting over 200 ms. This pattern is consistent with the classical result of an EPSP-IPSP sequence following electrical stimulation of thalamic afferents. However, the analysis cannot determine the time courses of EPSPs and IPSPs that overlap in time.

Voltage dependence

The relative time courses of the EPSPs and IPSPs that contribute to compound PSPs can be analyzed using the different voltage dependencies of EPSPs and IPSPs. Four control cells were studied at four membrane potentials ranging from -60 to -100 mV and used to estimate apparent reversal potentials (Fig. 4). Membrane

potentials were measured at 5-ms intervals between stimulus onset (30 ms) and the repolarization of the short latency IPSP (100 ms), and at 10-ms intervals after 100 ms. The mean apparent reversal is between -60 and -65 mV prior to stimulus onset (Fig. 5A). It reaches -57 mV at times corresponding to the peak of the depolarizing component of PSPs (20–30 ms after stimulus onset), but becomes more negative after 100 ms, reaching -70 mV at 400 ms. This analysis provides evidence for late inhibitory currents active after 100 ms. It does not, however, clarify whether or not early inhibitory currents are present in the 20–30 ms time window.

Extracellular application of bicuculline

The potential contribution of GABA_A-mediated currents to the early depolarizing PSPs was evaluated by bath application of bicuculline in six cells. Electrically evoked PSPs were recorded at 5-min intervals during the perfusion of bicuculline until a stable

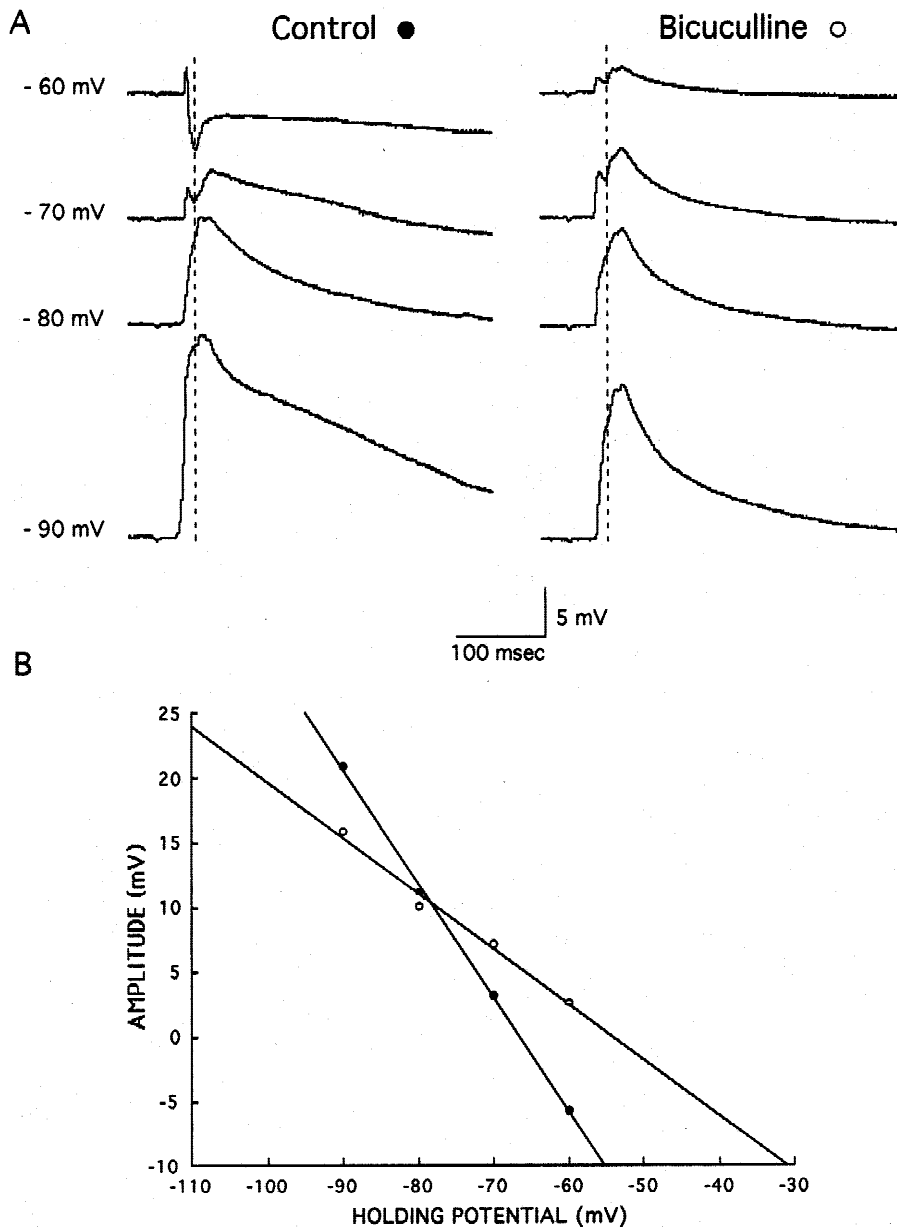


Fig. 4. Estimation of apparent reversal potentials. A: The amplitudes of PSPs were measured at the peak of the IPSP in control (filled circles) and at corresponding times in bicuculline (open circles) cells at four holding potentials. B: The amplitudes were plotted as a function of holding potential and fit with a linear equation to obtain the extrapolated reversal potential for the compound PSPs. Similar analyses were carried out at multiple time intervals throughout the response and used to create the plots in Fig. 5.

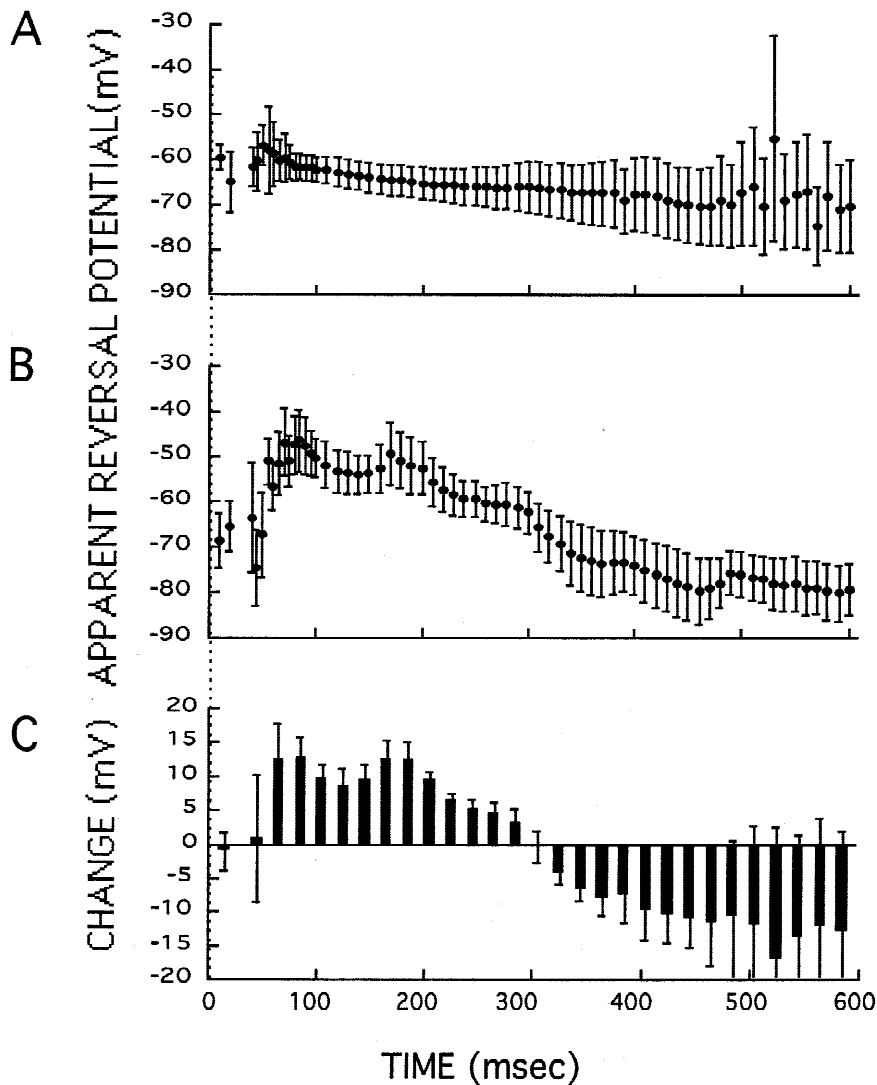


Fig. 5. The mean apparent reversal potential of four cells was measured at 10-ms intervals and plotted as a function of time. **A:** Apparent reversal potential of cells before the addition of 3.5 μ M bicuculline methiodide to the bathing solution. **B:** Apparent reversal potential of cells after the addition of bicuculline. **C:** Change of the mean apparent reversal potentials produced by the bath application of bicuculline plotted as a function of time.

response was attained. Cells with depolarizing potentials under control conditions showed an increase in PSP amplitude during the perfusion of bicuculline that was reduced to control levels after bicuculline was washed out (Fig. 6). PSPs obtained during the bath application of bicuculline were broad, depolarizing PSPs that often produced action potentials. They had a mean latency of 25.4 ± 0.9 ms, a mean peak time of 87.6 ± 8.1 ms, and a mean amplitude of 12.0 ± 1.6 mV. PSPs obtained after the application of bicuculline had latencies ($P = 0.03$), peak times ($P = 0.004$), and amplitudes ($P = 0.007$) that were significantly different from PSPs obtained under control conditions (Mann-Whitney test). Responses were depolarizing at all membrane potentials studied, including those in which control cells exhibited hyperpolarizations (Fig. 7).

Amplitudes of PSPs obtained by electrical stimulation at 2T were measured at several holding potentials and used to create plots of PSP peak amplitude as a function of holding potential in cells treated with bicuculline. The four cells used to obtain the apparent reversal potential at 10-ms intervals under control conditions were analyzed after the application of bicuculline

(Figs. 4 and 5B). The mean apparent reversal potential is depolarized by approximately 10 mV at 30 ms after stimulus onset, maintained depolarized for up to 300 ms and is then hyperpolarized after 300 ms (Fig. 5C). The initial shift of the apparent reversal potential in the depolarizing direction is consistent with the presence of an early IPSP that is masked by an EPSP. However, the biphasic response to extracellular bicuculline application is not consistent with a simple blockade of GABA_A receptor-mediated inhibition. This is not surprising since extracellular application of bicuculline not only blocks inhibition in the cell being recorded, but also disinhibits pyramidal cells and inhibitory interneurons throughout the cortex. The depolarization of the reversal potential early in the response could, thus, be due to a reduction of GABA_A receptor-mediated inhibition or an increased excitatory drive produced by disinhibition of reciprocally connected pyramidal cells. The hyperpolarization of the reversal potential late in the response could result from an increase in a GABA_B conductance, reflecting a reduction of inhibition to inhibitory interneurons.

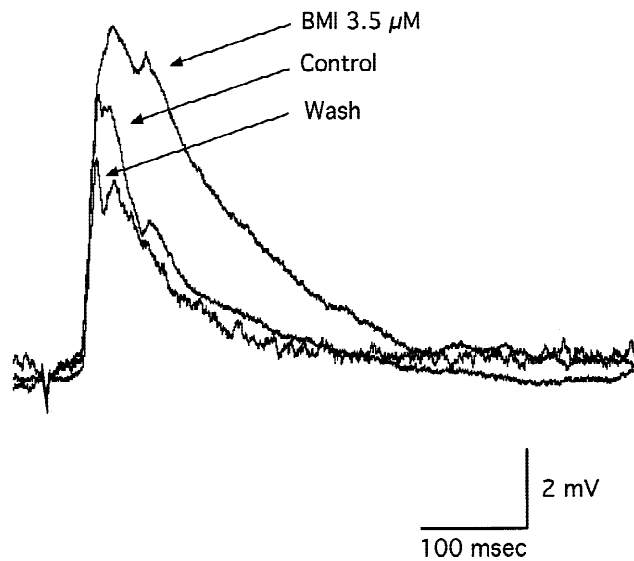


Fig. 6. Responses obtained before and after the application of $3.5 \mu\text{M}$ bicuculline methiodide in electrical-stimulation experiments. Traces obtained from a cell held at -65 mV . The trace obtained before the application of bicuculline (control) is smaller than the trace obtained after the bath application of bicuculline (BMI $3.5 \mu\text{M}$). The trace labeled "wash" was obtained after washing out the bicuculline for 1 h. Arrow indicates stimulus onset.

Intracellular perfusion of picrotoxin

Limiting the blockade of inhibition to the recorded cell by intracellular perfusion with the chloride channel blocker, picrotoxin, avoids the ambiguity in interpretation produced by the extracellular application of bicuculline and provides a way to study the contribution of GABA_A receptor-mediated inhibition to individual cells. In the following experiments, the responses of RS cells were studied after the passive perfusion of picrotoxin from the pipettes into the cells. Studies with picrotoxin perfusion do not have within-cell controls, so traces were obtained at a succession of times to follow the effects of picrotoxin perfusion from the pipette into the cell. Successful recordings were obtained in six cells. Fig. 8 shows three traces obtained from the same cell at different times after impalement. The amplitudes of electrically evoked PSPs increase as a function of time following impalement. PSPs obtained following intracellular application of picrotoxin are complex depolarizations that can last up to 800 ms. There is a notable increase in the excitability of cells demonstrated by the trace obtained after 2.5 h of perfusion which shows more action potentials than the trace obtained at 21 min of perfusion. PSPs had a mean latency of $21.0 \pm 1.5 \text{ ms}$, a mean peak time of $98.5 \pm 13.4 \text{ ms}$, and a mean amplitude of $7.8 \pm 0.7 \text{ mV}$. Peak times of PSPs obtained after the perfusion of picrotoxin are significantly longer than peak times of PSPs obtained under control conditions ($P = 0.009$, Mann-Whitney test). Traces from four cells held at

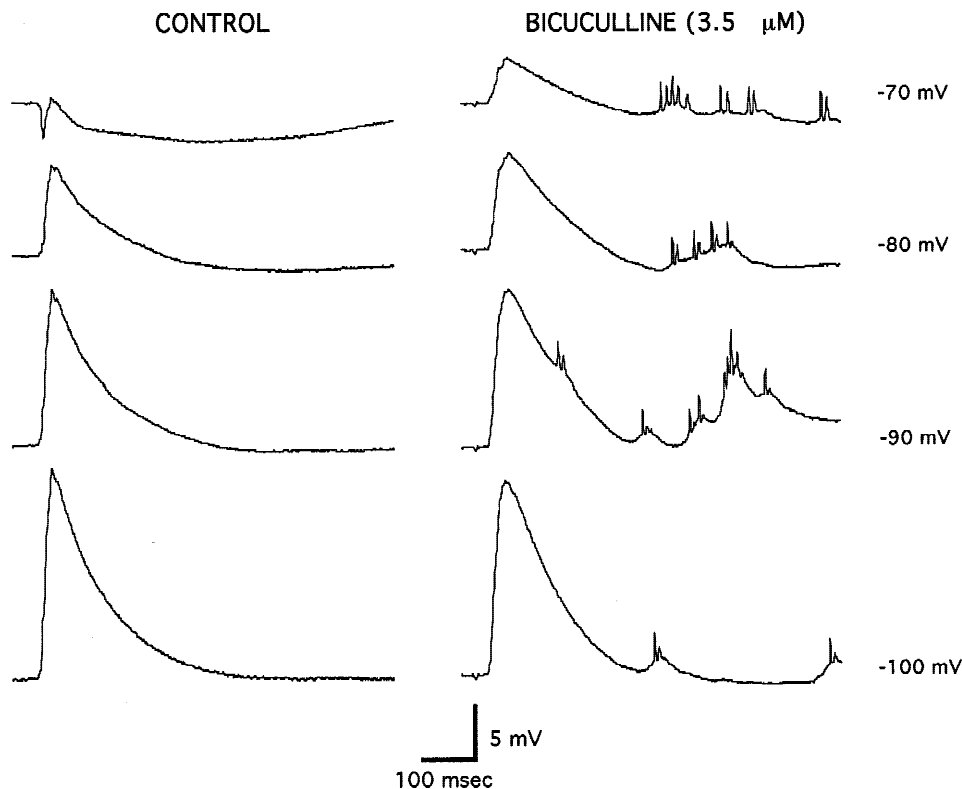


Fig. 7. Voltage responses of an RS cell stimulated at $2T$ and recorded at different holding potentials before (control) and after (bicuculline) the bath application of $3.5 \mu\text{M}$ bicuculline methiodide. At rest (-70 mV), the control response is biphasic with an early hyperpolarization and a later depolarization. At negative holding potentials, the hyperpolarization is not seen and the depolarization increases in amplitude. The bicuculline responses do not show the early hyperpolarization at -70 mV and have broader PSPs that also increase in amplitude at negative holding potentials. Note the increased number of action potentials in the bicuculline responses. Action potentials are truncated because the traces are averages of 20 responses.

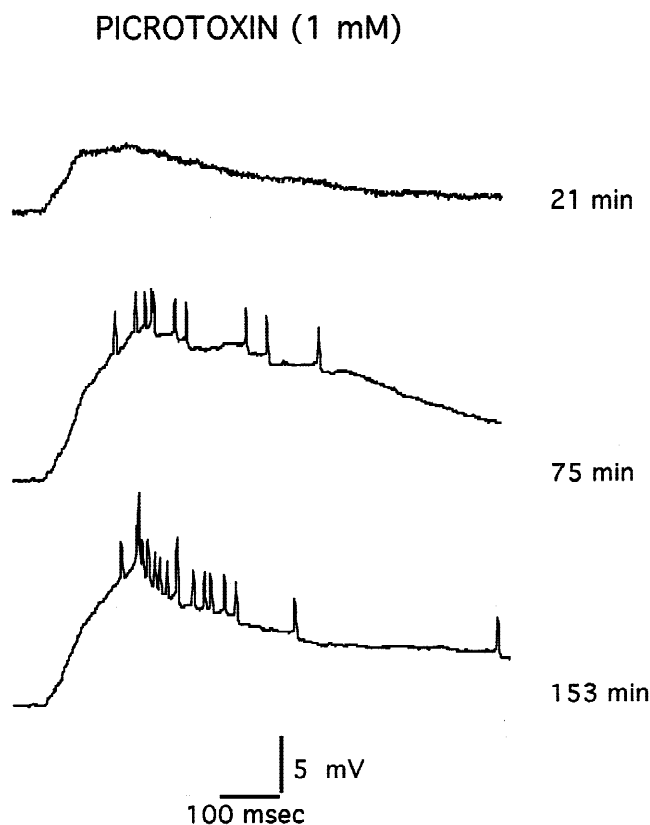


Fig. 8. Intracellular perfusion with picrotoxin. Traces obtained from a cell at different times after impalement with an intracellular pipette containing 1 mM picrotoxin in 4 M potassium acetate. There is an increase in the amplitude and excitability of responses with increasing perfusion times. Action potentials are truncated because the traces are averages of 20 responses.

–60 mV and stimulated at $2T$ were used to create a plot of mean amplitude as a function of time (Fig. 9A). This plot focuses on the rising phase of the PSPs produced by picrotoxin. The increase can be better seen in Fig. 9B, which shows the slope of the mean amplitude plotted at 10-ms intervals for control and picrotoxin-treated cells. The slope is larger in picrotoxin-treated cells between 20 and 30 ms after stimulus onset, suggesting an involvement of GABA_A receptor-mediated inhibition at times corresponding to the latency of control PSPs (22.7 ± 0.6 ms).

Light-evoked PSPs

General features

Light-evoked PSPs were described in detail by Mancilla et al. (1998). Briefly, light-evoked PSPs are composed of depolarizing potentials of varying amplitudes. They increase in amplitude with increasing light intensity until reaching a maximum at a light intensity of about 200–400 photons $\mu\text{m}^{-2} \text{s}^{-1}$. Responses at higher light intensities vary considerably in amplitude, but tend to fall below the maximum amplitude.

Voltage dependence

Light-evoked PSPs were recorded at several different holding potentials in four cells. Membrane potentials were measured at

10-ms intervals in these cells and used to plot mean apparent reversal potential as a function of time (Fig. 10). The mean apparent reversal potential is approximately equal to the mean resting membrane potential of the four cells until 140 ms following the light flash. It then shifts in the hyperpolarizing direction, reaching approximately –68 mV between 190 and 250 ms following light onset. It returns to the resting membrane potential by about 300 ms following light onset. This is consistent with activation of inhibitory currents beginning about 150 ms after light onset. The relative magnitudes of the inhibitory and excitatory currents will, however, vary as a function of the membrane potential. Inhibitory currents will make a relatively small contribution to the total synaptic current while the cell is near its resting membrane potential (which is near the reversal potential for GABA_A receptor-mediated currents), so that activation of inhibitory and excitatory synapses result in a depolarizing PSP.

Intracellular perfusion of picrotoxin

Light responses (Fig. 11) were obtained in 11 cells perfused with picrotoxin, seven of which had responses at enough light intensities to construct IR functions. Three had more than one light series, resulting in a total sample of ten sets of light responses. Five light responses from three cells under control conditions and four light responses from three cells after the perfusion of picrotoxin were used to create a plot of the mean amplitude of control (closed circles) and picrotoxin (open circles) responses as a function of time (Fig. 12). Responses were obtained at an intensity of 172 photons $\mu\text{m}^{-2} \text{s}^{-1}$ (which is below the intensity at which most RS cells produce action potentials under control conditions) to minimize the contribution of feedback inhibition to the responses used for the mean amplitude plots. The plot shows that the light responses of cells perfused with picrotoxin become larger than those of control cells 300 ms after the light is turned on, and are maintained elevated until 700 ms after the light is turned off.

The amplitudes of light-evoked PSPs were measured at different intensities of light and plotted as IR functions (Fig. 13). IR functions had I_{50} values of 128 ± 3.2 photons $\mu\text{m}^{-2} \text{s}^{-1}$, k values of 1.6 ± 0.6 , R_{max} values of 16.1 ± 1.7 mV, and threshold values of 130.9 ± 2.5 photons $\mu\text{m}^{-2} \text{s}^{-1}$. The only value that was significantly different ($P = 0.003$, Mann–Whitney test) between control and picrotoxin light responses was R_{max} , which was 8.2 ± 1.2 mV for the control responses. The latency of the light responses in cells obtained with picrotoxin in the intracellular pipette was measured at different intensities to create plots of mean population latency as a function of light intensity (Fig. 14A). The latencies of the picrotoxin cells were significantly longer than those of control cells during the rising phase of the IR curves ($P = 0.006$ – 0.05 , Mann–Whitney test), but not significantly different at all other intensities tested. Peak times in picrotoxin cells were not significantly different than peak times in control cells (Fig. 14B).

In the control population (Mancilla et al., 1998), five out of 15 RS cells produced action potentials at one or more intensities of light. Four of the cells produced action potentials at fewer than two intensities. In contrast, six out of 11 picrotoxin cells produced action potentials at one or more intensities of light. Four produced action potentials at more than three intensities, with one producing action potentials at 14 different intensities. Like the control population, the majority of cells treated with picrotoxin produced only one action potential during the light response (Fig. 10). The mean latency to the first action potential for picrotoxin cells is 552 ± 27 ms, which is not significantly different from that of control cells (639 ± 64 ms).

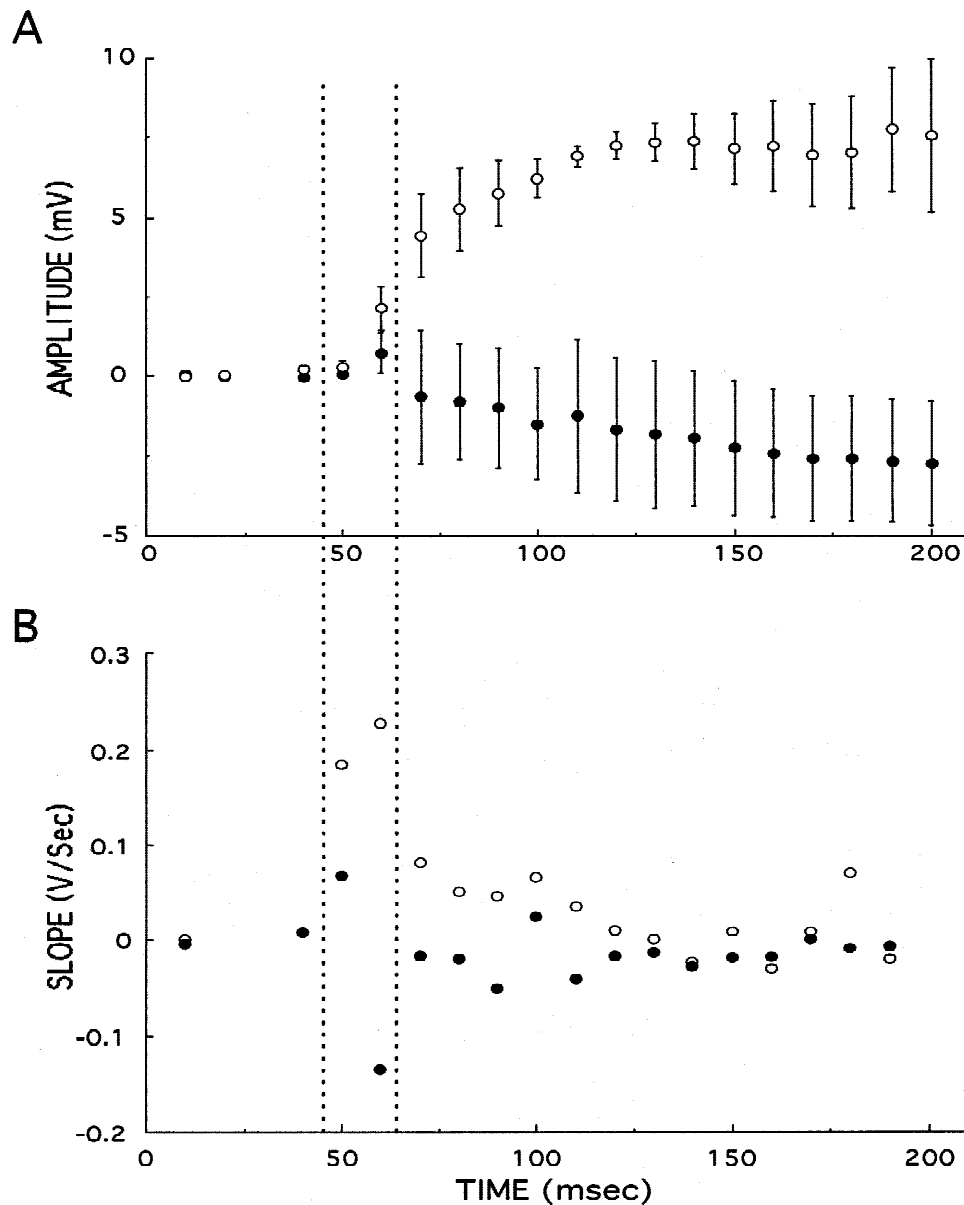


Fig. 9. Effects of intracellular perfusion with picrotoxin on electrically evoked PSPs. A: The mean amplitude of control responses are compared to the mean amplitudes of responses obtained from four cells impaled with a pipette containing 1 mM picrotoxin. Responses from cells impaled with picrotoxin-containing pipettes were obtained by stimulating the LFB at the same intensity and holding cells at the same membrane potential (-60 mV) as control cells. Responses obtained with picrotoxin in the pipettes were depolarizing PSPs that had larger amplitudes than the responses obtained from control cells. B: The slopes of the mean amplitude plots were calculated at 10-ms intervals to obtain a plot of the slope of the mean amplitude of control (closed circles) and picrotoxin (open circles) cells as a function of time. Dashed lines indicate the time at which the slope of the mean amplitude plot of picrotoxin cells is larger than that of controls. Measurements obtained at 30 ms were omitted to eliminate the stimulus artifact from the plot.

Discussion

The experiments reported here provide evidence for early and late inhibition in RS cells following activation by both electrical and light stimulation.

Electrically evoked PSPs

PSPs obtained from RS cells in turtle visual cortex by electrical stimulation of thalamocortical afferents resemble those obtained

by Larson-Prior et al. (1991) and Colombe and Ulinski (1999) in the same preparation. The EPSP-IPSP sequences observed here were observed in 64.8% of the responses of cells to optic nerve stimulation (Pivovarov & Trepakov, 1972), while IPSPs without preceding EPSPs were seen in 6.8% of responses. IPSPs without EPSPs were also seen following electrical stimulation of the superficial molecular layer of the cortex by Kriegstein and Connors (1986). PSPs in turtle visual cortex are similar to PSPs obtained when the optic tract (Watanabe et al., 1966; Ferster & Lindström,

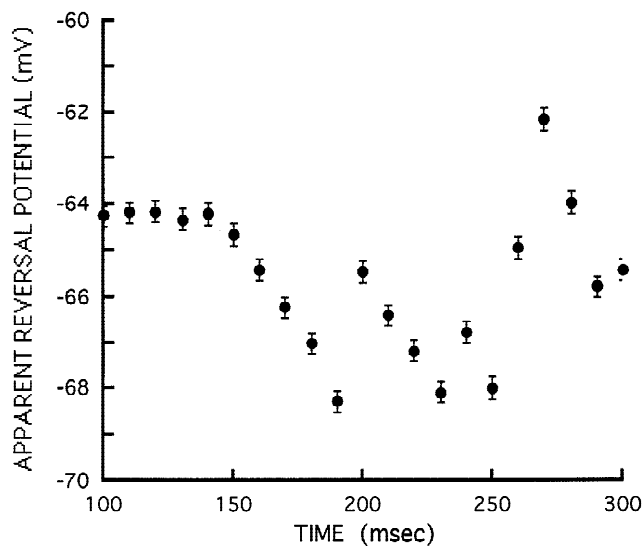


Fig. 10. Mean apparent reversal potentials of light-evoked responses. Amplitudes of light-evoked responses were measured at four different holding potentials at 10-ms intervals and used to estimate apparent reversal potentials in four cells. Averages for the four cells are plotted at each time point to produce a curve showing the mean apparent reversal potential as a function of time during the 100–300 ms time interval. There is a clear shift in apparent reversal potential in the hyperpolarizing direction beginning at 140 ms.

1983), optic radiation (Watanabe et al., 1966; Ferster & Lindström, 1983), lateral geniculate body (Li et al., 1960; Ferster & Lindström, 1983), dorsal columns (Anderson, 1965), skin (Anderson, 1965), or ventral posterior nucleus (Li, 1963; Contreras et al., 1997) are stimulated in cat. They are also similar to those obtained when the medial geniculate (Metherate & Ashe, 1994) or the ventrolateral nucleus (Castro-Alamancos & Connors, 1996) are stimulated in rats, or when the ventrobasal nucleus is stimulated in mice (Gil & Amitai, 1996). IPSPs follow monosynaptic EPSPs, or are produced without preceding EPSPs, in all the PSPs produced by thalamic stimulation.

Extracellular application of bicuculline

Bicuculline blocks early IPSPs in cortical neurons (Connors et al., 1988; Chagnac-Amitai & Connors, 1989) and has been used to study the contribution of inhibition to the receptive-field properties of cortical cells. Iontophoretic application of bicuculline to the primary visual cortex of cat changes the ocular dominance (Sillito et al., 1980), end inhibition (Sillito & Versiani, 1976), velocity tuning (Patel & Sillito, 1978), spatial-frequency tuning (Vidyasagar & Mueller, 1994), orientation tuning (Sillito, 1975, 1979; Eysel & Shevelev, 1994), and direction selectivity (Sillito, 1975, 1977; Tsumoto et al., 1979; Nelson, 1991; Sato et al., 1995) of cells. A broadening of orientation tuning after the application of bicuculline has also been seen in cells of the macaque visual cortex (Sato et al., 1996). In the somatosensory cortex of cat, iontophoretic application of bicuculline increases receptive-field size (Hicks & Dykes, 1983; Dykes et al., 1984; Alloway et al., 1989; Batuev et al., 1988, 1989) and reduces direction selectivity (Batuev et al., 1988, 1989) of rapidly adapting units. The same change in receptive-field size and direction selec-

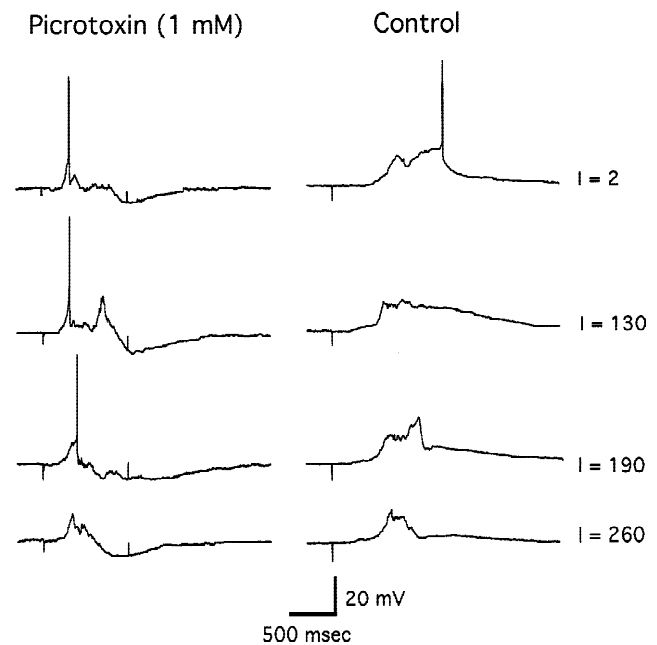


Fig. 11. Effect of picrotoxin perfusion on light-evoked PSPs. Light responses obtained at a holding potential of -65 mV from a cell impaled with a pipette containing 1 mM picrotoxin and from a control cell. Traces are responses to a single-stimulus presentation. The onset and offset of the 640-nm light flash is marked by the stimulus artifacts at 300 ms and 1300 ms. Light intensities (I) are given in 10^2 photons $\mu\text{m}^{-2} \text{s}^{-1}$.

tivity after the application of bicuculline is seen in RS units of the rat somatosensory cortex (Kyriazi et al., 1996). The changes in receptive-field properties observed with bicuculline suggests that inhibition is tuning the receptive-field properties of cortical cells by reducing responses to nonoptimal stimuli.

However, experiments that rely upon extracellular application of bicuculline can be difficult to interpret. Bicuculline applied iontophoretically with ejection currents of 2–80 nA, from pipettes with tip diameters of 2–4 μm , has been estimated to affect cells within a 200- μm radius (Sato et al., 1995). Using the cell-density measurements of Beaulieu and Colonnier (1983) for layer IV in cat visual cortex, a sphere with a radius of 200 μm contains 2145 cells. Extracellular application of bicuculline can, therefore, block GABA_A receptors on approximately 2000 excitatory and inhibitory cells throughout the neighborhood of the recording pipette, producing complex effects on the recorded cell. Consistent with this, analysis of the reversal potential at 10-ms intervals shows a change in the reversal potential between control and bicuculline responses at times corresponding to the peak of the early depolarization. This change could be due to an involvement of GABA_A-mediated inhibition at these times. However, the change in reversal potential could also be due to an increase of reexcitation. The long latency depolarizations seen in traces obtained from cells during the bath application of bicuculline suggest the presence of increased reexcitation. An increase in reexcitation with the application of bicuculline has also been seen in intracellular recordings of layer II/III RS cells in the sensorimotor cortex (Hwa & Avoli, 1992) and in field potentials of the auditory cortex of rat (Metherate & Ashe, 1994). Whether the reexcitation is increased earlier in the response is difficult to determine from these experiments.

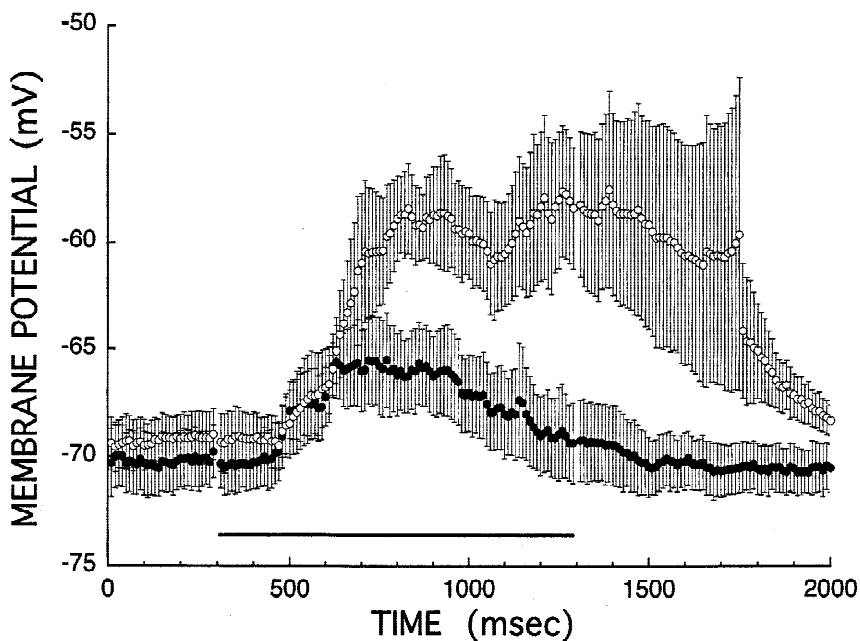


Fig. 12. Effects of picrotoxin perfusion on amplitudes of light-evoked PSPs. Amplitudes of light-evoked PSPs from five traces in three control cells and four traces in three cells impaled with pipettes containing picrotoxin were measured at 10-ms intervals to create a plot of the mean amplitudes of control (closed circles) and picrotoxin (open circles) cells as a function of time. The bar at the bottom indicates the time during which the diffuse light was on.

Intracellular perfusion of picrotoxin

Ambiguity in interpretation created by bath application of GABA_A antagonists can be avoided by perfusing cells intracellularly with the selective chloride channel blocker, picrotoxin (Masumi & Akaike, 1988; ffrench-Constant et al., 1993a,b; Xu et al., 1995). Picrotoxin blocks GABA_A currents when applied either extracellularly (Gallagher et al., 1978; Akaike et al., 1985; Maksay & Ticku, 1985; Kriegstein, 1987; Smart & Constanti, 1986; Yakushiji et al., 1987; Inoue & Akaike, 1988; Newland & Cull-Candy, 1992;

ffrench-Constant et al., 1993a,b; Yoon et al., 1993; Macdonald & Olsen, 1994) or intracellularly (Akaike et al., 1985; Metherate & Ashe, 1993; Nelson et al., 1994). In addition, applying picrotoxin to the inside surface of inside-out patches blocks GABA- and pentobarbital-mediated chloride currents (Akaike et al., 1985; Inomata et al., 1988).

The mechanism by which intracellular application of picrotoxin blocks GABA currents is not certain, but extracellularly applied picrotoxin likely binds to the open channel to produce a noncompetitive block of GABA currents (Gallagher et al., 1978; Akaike et al., 1985; Yakushiji et al., 1987; Inoue & Akaike, 1988) that increases in effectiveness with GABA pretreatment (Inoue & Akaike, 1988; Newland & Cull-Candy, 1992; Yoon et al., 1993). Mutations in the pore lining region of the M2 segment of the GABA_A receptor complex affect the binding of picrotoxin (ffrench et al., 1993a,b; Xu et al., 1995), which is thought to be small enough to reach the binding site in the M2 segment from the extracellular surface (Xu et al., 1995). It is not known whether intracellularly applied picrotoxin reaches this binding site by entering the open channel from the inside or crossing the membrane and entering the channel from the outside.

Although intracellular perfusion of picrotoxin can be a valuable tool for assessing GABA_A receptor-mediated inhibition in the recorded cell, there are at least two caveats. First, the extent to which picrotoxin perfuses into the dendrites of the neuron is not known, precluding any conclusion about the percentage of GABA_A receptors blocked. An attempt was made in our studies to find a concentration of picrotoxin that produced a stable change in evoked PSPs, but the effects demonstrated should be considered minimal effects rather than demonstrating the complete effect of removing GABA_A receptor-mediated inhibition. Second, picrotoxin is a low-molecular-weight, uncharged plant toxin that could cross the membrane and diffuse away from the cell to produce a blockade of receptors on neighboring cells. The extent to which picrotoxin crosses the membrane is difficult to ascertain, but it is likely that the blockade of GABA_A receptors is much more localized than

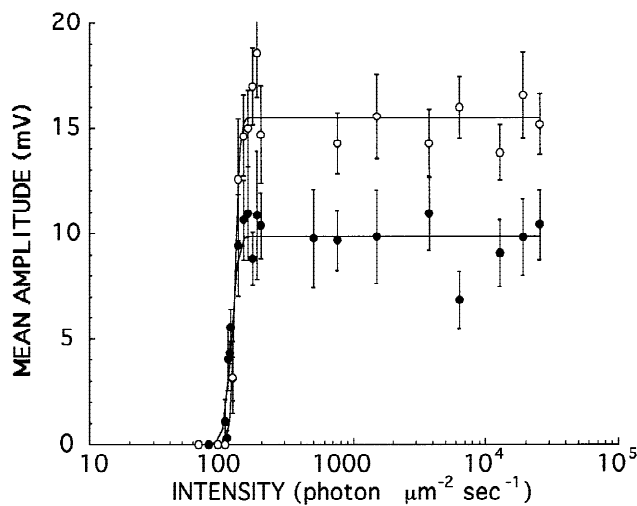


Fig. 13. Effects of picrotoxin perfusion on intensity–response functions. Intensity–response function obtained by measuring the mean amplitude of responses from cells impaled with pipettes containing 1 mM picrotoxin (open circles) and control (closed circles) cells. The IR curves were fit with Boltzmann functions.

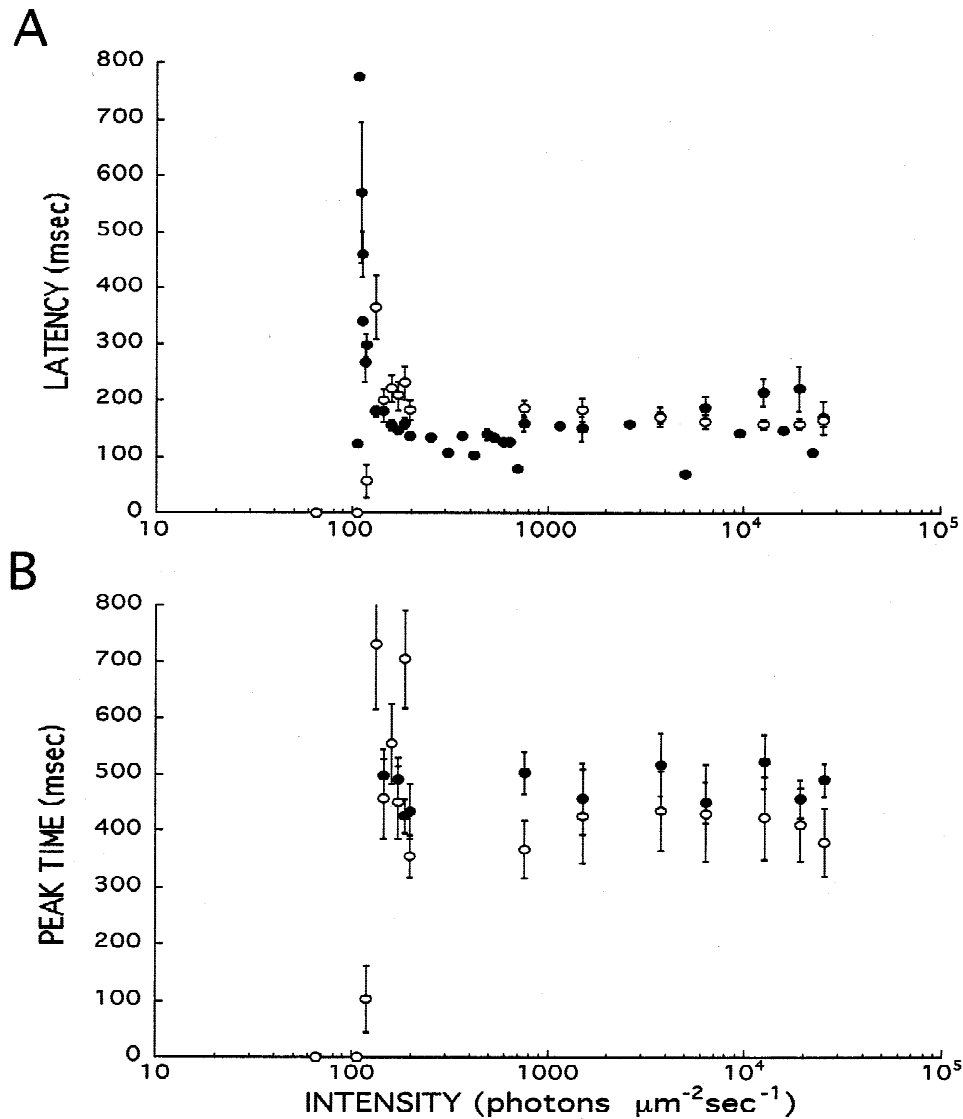


Fig. 14. Effects of picrotoxin perfusion on the latencies and times to peak of light-evoked PSPs. A: Mean latencies of light responses of control cells (filled circles) are compared to the mean latencies of light responses obtained with 1 mM picrotoxin in the intracellular pipettes (open circles). The latencies of the light responses of cells impaled with picrotoxin in the pipettes are significantly different from controls at intensities that correspond to the rising phase of IR curves only ($P = 0.006\text{--}0.05$, Mann-Whitney test). B: Mean peak times of light responses of control cells (filled circles) are compared to the mean peak times of light responses obtained from cells impaled with 1 mM picrotoxin in the pipettes (open circles). Mean peak times of responses obtained from cells impaled with picrotoxin in the pipettes are not significantly different than controls.

with iontophoretic or bath application of bicuculline. The flow from a pipette is proportional to the cube of the tip radius (Krnjevic et al., 1963; Purves, 1981), and should be even less for intracellular pipettes with resistances of 100–150 M Ω than for iontophoretic pipettes with resistances of 10–50 M Ω (Douglas & Martin, 1991). Krnjevic et al. (1963) found that a 10-fold change in pipette resistance produced a 100-fold change in spontaneous release of acetylcholine. Thus, the amount of picrotoxin crossing the cell membrane is likely to be more than 100 times less than that applied extracellularly.

Intracellular perfusion of picrotoxin produced an increase in the amplitudes of electrically evoked PSPs in turtle RS cells. Like PSPs produced in cells during the extracellular application of bicuculline, the PSPs produced in cells perfused internally with pi-

crotoxin are depolarizing at -60 mV. Metherate and Ashe (1993) obtained similar results in the auditory cortex of rats. They used patch-clamp electrodes to internally perfuse cells with the potassium channel blocker, cesium, combined with 10 μM picrotoxin. This combination of blockers produced spontaneous, large amplitude depolarizations which led to bursts of action potentials. The amplitude of high-frequency fluctuations produced by nucleus basalis stimulation was also increased. Nelson et al. (1994) found an increase in the amplitude of PSPs in cat primary visual cortex after the establishment of whole-cell recordings with patch pipettes containing 1 mM picrotoxin and cesium. The inhibition produced by turning on a light bar in the OFF subfield or turning off the bar in the ON subfield of receptive fields of simple cells was blocked by perfusion of the blockers.

Time course of inhibition

Electrical stimulation of thalamic afferents produced relatively stereotyped PSPs with a mean latency of 22.7 ± 0.6 ms that is comparable to the mean latency (21 ± 4 ms) obtained by Larson-Prior et al. (1991). PSPs overlap in time with the earliest effects attributable to inhibitory currents observed as a change in reversal potential or a change in the slope of responses after the blockade of inhibition. There is a 10-mV change in the reversal potential 30 ms after stimulus onset after the bath application of bicuculline. In cells perfused with picrotoxin, the mean slope is larger than that of control cells between 20 and 30 ms after stimulus onset. PSPs obtained from RS cells impaled with pipettes containing picrotoxin are broader than those obtained under control conditions and have amplitudes that are maintained above those of control cells for approximately 800 ms. Electrical stimulation of thalamic afferents, thus, produces inhibition that overlaps with the earliest effects of geniculocortical excitation and lasts throughout the response.

Light flashes evoke compound PSPs in RS cells with latencies that range between 158–221 ms (Mancilla et al., 1998). The mean light response obtained for control cells during the rising phase of the IR curve had a latency of approximately 180 ms and a duration of about 1 s. The time course of light responses in cortical cells reflects variability of responses at the retinal level. Light flashes to the dark-adapted retina activate both cones and rods which produce responses in ganglion cells with different latencies (Baylor & Fettiplace, 1977; Bowling, 1980). Ganglion cell responses due to cone activation have latencies between 100–300 ms while responses due to rod activation have latencies beyond 400 ms (Bowling, 1980). Additional variability is introduced by differences in the duration of responses of ganglion cells. Most ganglion cell responses to a stationary light flash are transient, but 5–8% of ganglion cells respond vigorously throughout the duration of the stimulus (Bowling, 1980; Granda & Fulbrook, 1989), and about half have weaker maintained discharges of 0.2–2.0 impulses/s (Bowling, 1980).

The plot of the mean light responses of control and picrotoxin cells shows that the initial slope of both responses is similar, but diverges at about 300 ms after light onset or 150 ms after the onset of the compound PSP. Light responses under control conditions reach a plateau at this time, but the slope of the light responses of picrotoxin cells increases further until reaching a maximum around 600 ms after light onset. The mean amplitude of responses in picrotoxin cells is maintained above the mean amplitude of control cells for approximately 1.5 s. One interpretation of these data is that RS cells do not receive significant inhibition before 300 ms after light onset. However, the firing times of FS cells is maximal between 200–300 ms after light onset, indicating that RS cells should receive the greatest inhibition at these times. A possible explanation for the apparent lack of inhibition between 200–300 ms is that the resting membrane potential of RS cells is often close to the reversal potential for the early IPSPs. There would, consequently, be little driving potential for inhibition until a significant amount of excitation has accumulated. This is consistent with the shift in apparent reversal potentials of light-evoked PSPs in the hyperpolarizing direction between 140 and 300 ms after light onset. This shift could result from a net hyperpolarizing current generated by GABA_A-mediated inhibition with a reversal potential near -70 mV. The voltage dependency of light-evoked PSPs, thus, provides evidence for early inhibition in light-evoked PSPs while the picrotoxin experiments provide evidence for late inhibition.

Feedforward vs. feedback inhibition

Determining the contributions of feedforward and feedback inhibition in RS cells is technically difficult in both turtles and mammals because it depends upon analysis of very short latency effects. In mammals, the latency of disynaptic potentials is about 0.8 ms longer than that of monosynaptic potentials, while in cold blooded vertebrates the difference is generally between 0.5–1 ms (Berry & Pentreath, 1976). This difference is smaller than the 10–90% rise time found for unitary EPSPs in turtle visual cortex (0.7–22.5 ms) by Mancilla and Ulinski (1995) and the 10–90% rise time found for thalamocortical EPSPs in layer V pyramidal cells of mouse somatosensory cortex (4.93 ± 2.84 ms) by Gil and Amitai (1996). This suggests that disynaptic IPSPs can occur early enough to control the amplitudes of unitary EPSPs in cortical cells in both turtles and mammals. Transient changes in luminance would, then, produce feedforward inhibitory and excitatory signals that reach the cortex with roughly the same latency. Since luminance changes produce asynchronous and on-going trains of action potentials in retinal ganglion cells, the small difference in latency which results from the presence of an additional synaptic delay with electrical activation is irrelevant with natural stimuli. Although there are small differences in the latencies of PSPs in RS and FS cells with natural stimuli, FS cells produce action potentials on the order of 200 ms before RS cells do. Disynaptic IPSPs can, then, play a potentially significant role in regulating the production of monosynaptic EPSPs. These effects would be mediated by a pure feedforward inhibition which is operative during the rising phase of the PSPs.

The situation later in the response is more complex. Even brief changes in luminance can produce prolonged trains of action potentials in retinal ganglion cells (Marchiafava, 1983), so PSPs evoked by spikes late in the train will overlap with responses evoked for the first few spikes in the train. These responses likely include contributions from feedback processes, since activation of even a fraction of pyramidal cells by feedforward excitatory pathways will result in recurrent excitation within the cortex *via* the collaterals of pyramidal cells, which overlap with the time course of the excitatory drive from geniculate afferents. Similarly, visual stimuli above the threshold for pyramidal cell activation will produce IPSPs in pyramidal cells that result from both layer 1 and layer 3 inhibitory interneurons.

The only parameter that is significantly different between control IR curves and IR curves obtained from cells perfused with picrotoxin is the maximum amplitude. The fact that the threshold intensity did not change suggests that it is set by the convergence of inputs along the visual pathway and is not a consequence of intracortical mechanisms (Mancilla et al., 1998). Similarly, the fact that the I_{50} and k values obtained for the control cells and the cells treated with picrotoxin are not different suggests that both IR curves have similar rising phases. The rising phase leads to a saturation phase that occurs at the same intensities regardless of the level of inhibition, suggesting that the saturation of IR curves is not a consequence of intracortical inhibition and is probably due to saturation occurring earlier in the visual pathway. IR functions of ganglion cells already exhibit saturation (Marchiafava, 1983) and could limit the amount of excitation reaching the cortex. Similarly, the shapes of contrast–response functions in simple and complex cells of cat visual cortex were unchanged by the iontophoretic application of bicuculline (DeBruyn & Bonds, 1986). These findings suggest that the shapes of IR curves in turtle visual cortex and contrast–response functions in cat visual cortex might be set by subcortical mechanisms.

Strategies of inhibition

The picture of the functional role of intracortical inhibition that comes from our work differs in several important ways from the model proposed by Douglas, Martin, and their colleagues (Douglas & Martin, 1991; Douglas et al., 1995; Suarez et al., 1995). They estimate that thalamic afferents provide 5% of the excitation upon cortical spiny cells (Ahmed et al., 1994), and hypothesize that the feedforward gain of the geniculocortical pathway is relatively low. The feedforward signal, consequently, requires amplification by recurrent excitation in order to have an effect upon the firing probabilities of cortical neurons. In their model, inhibition plays little or no role in regulating the feedforward gain, but is required to stabilize the massive recurrent excitation needed to amplify the input signal. Suarez et al. (1995) suggest that the cortical circuit resembles a proportional amplifier in its design.

By contrast, Mancilla et al. (1998) directly measured the gain of the geniculocortical pathway with the *in vitro* turtle preparation. The gain is quite high, so an average of about 500 photons $\mu\text{m}^{-2} \text{s}^{-1}$ can bring a cortical pyramidal cell to its firing threshold. Consistent with this, action potentials in FS cells are timed to produce maximal inhibition during the rising phases of thalamocortical EPSPs, as demonstrated by experiments in which blocking inhibition with picrotoxin increases the slope of EPSPs. Since RS cells often have resting membrane potentials close to the chloride reversal potential, feedforward inhibition may not have a visible effect until a sequence of EPSPs has depolarized the cell enough to create a large driving potential for IPSPs. GABA_A receptor-mediated intracortical inhibition regulates the amplitudes of light-evoked EPSPs in RS cells, but does not appear necessary to stabilize the cortical circuitry since the overall shape of the IR curve appears to be determined largely by retinal or geniculate mechanisms. Inhibition in cortical circuits appears to act as a brake timed to overlap with both monosynaptic and polysynaptic EPSPs.

Acknowledgments

Parts of this work were supported by a PHS grant from The National Eye Institute and an NSF grant from The Learning and Intelligent Systems Program at the National Science Foundation. J.G. Mancilla was supported by a GMS training grant to the Committee on Neurobiology at the University of Chicago.

References

- AHMED, B., ANDERSON, J.C., DOUGLAS, R.J., MARTIN, K.A.C. & NELSON, J.C. (1994). Polynuclear innervation of spiny stellate neurons in cat visual cortex. *Journal of Comparative Neurology* **341**, 39–49.
- AKAIKE, N., HATTORI, K., OOMURA, Y. & CARPENTER, D.O. (1985). Bicuculline and picrotoxin block γ -aminobutyric acid-gated Cl^- conductance by different mechanisms. *Experientia* **41**, 70–71.
- ALLOWAY, K.D., ROSENTHAL, P. & BURTON, H. (1989). Quantitative measurements of receptive field changes during antagonism of GABAergic transmission in primary somatosensory cortex of cats. *Experimental Brain Research* **78**, 514–532.
- ANDERSON, S.A. (1965). Intracellular postsynaptic potentials in the somatosensory cortex of the cat. *Nature* **205**, 297–298.
- ANDERSON, J.C., DOUGLAS, R.J., MARTIN, K.A.C. & NELSON, J.C. (1994). Map of the synapses formed with the dendrites of spiny stellate neurons of cat visual cortex. *Journal of Comparative Neurology* **341**, 25–38.
- AZOUZ, R., GRAY, C.M., NOWAK, L.G. & MCCORMICK, D.A. (1997). Physiological properties of inhibitory interneurons in cat striate cortex. *Cerebral Cortex* **7**, 534–545.
- BATUEV, A.S., ALEKSANDROV, A.A., SHCHEYNIKOV, N.A., KHARAZIYA, V.N. & CHAN, T.C. (1988). Role of inhibitory processes in shaping functional characteristics of neurons of the vibrissae projection area of the somatosensory cortex in the cat. *Neuroscience Behavior Physiology* **18**, 222–230.
- BATUEV, A.S., ALEKSANDROV, A.A., SHCHEYNIKOV, N.A., KCHARAZIA, V.N. & AN, C.C. (1989). The role of inhibitory processes in the formation of functional properties of neurons in vibrissal projection zone of the cat somatosensory cortex. *Experimental Brain Research* **76**, 198–206.
- BAYLOR, D.A. & FETTLPLACE, R. (1977). Kinetics of synaptic transfer from receptors to ganglion cells in turtle retina. *Journal of Physiology (London)* **271**, 425–448.
- BEAULIEU, C. & COLONNIER, M. (1983). The number of neurons in the different laminae of the binocular and monocular regions of area 17 in the cat. *Journal of Comparative Neurology* **217**, 337–344.
- BERRY, M.S. & PENTREATH, V.W. (1976). Criteria for distinguishing between monosynaptic and polysynaptic transmission. *Brain Research* **105**, 1–20.
- BLANTON, M.G. & KRIEGSTEIN, A.R. (1991). Spontaneous action potential activity and synaptic currents in the embryonic turtle cerebral cortex. *Journal of Neuroscience* **11**, 3907–3923.
- BLANTON, M.G. & KRIEGSTEIN, A.R. (1992). Properties of amino acid neurotransmitter receptors of embryonic cortical neurons when activated by exogenous and endogenous agonists. *Journal of Neurophysiology* **67**, 1185–1200.
- BOWLING, D.B. (1980). Light responses of ganglion cells in the retina of the turtle. *Journal of Physiology (London)* **299**, 173–196.
- CASTRO-ALAMANCOS, M.A. & CONNORS, B.W. (1996). Cellular mechanisms of the augmenting response: Short-term plasticity in a thalamocortical pathway. *Journal of Neuroscience* **16**, 7742–7756.
- CAULI, B., AUDINAT, E., LAMOLEZ, B., ANGULO, M.C., ROPERT, N., TSUZUKI, K., HESTRIN, S. & ROSSIER, J. (1997). Molecular and physiological diversity of cortical nonpyramidal cells. *Journal of Neuroscience* **17**, 3894–3906.
- CHAGNAC-AMITAI, Y. & CONNORS, B.W. (1989). Synchronized excitation and inhibition driven by intrinsically bursting neurons in neocortex. *Journal of Neurophysiology* **62**, 1149–1162.
- CHEN, W., ZHANG, J.J., HU, G.Y. & WU, C.P. (1996). Electrophysiological and morphological properties of pyramidal and nonpyramidal neurons in the cat motor cortex *in vitro*. *Neuroscience* **73**, 39–55.
- COLOMBE, J.B. & ULINSKI, P.S. (1999). Temporal dispersion windows in cortical neurons. *Journal of Computational Neuroscience* **7**, 71–87.
- CONNORS, B.W., GUTNICK, M.J. & PRINCE, D.A. (1982). Electrophysiological properties of neocortical neurons *in vitro*. *Journal of Neurophysiology* **48**, 1302–1320.
- CONNORS, B.W. & KRIEGSTEIN, A.R. (1986). Cellular physiology of the turtle visual cortex: Distinctive properties of pyramidal and stellate neurons. *Journal of Neuroscience* **6**, 164–177.
- CONNORS, B.W. & GUTNICK, M.J. (1990). Intrinsic firing patterns of diverse neocortical neurons. *Trends in Neuroscience* **13**, 99–104.
- CONNORS, B.W., MALENKA, R.C. & SILVA, L.R. (1988). Two inhibitory postsynaptic potentials, and GABA_A and GABA_B receptor-mediated responses in neocortex of rat and cat. *Journal of Physiology* **406**, 443–468.
- CONTRERAS, D., DESTEXHE, A. & STERIADE, M. (1997). Intracellular and computational characterization of the intracortical inhibitory control of synchronized thalamic inputs *in vivo*. *Journal of Neurophysiology* **78**, 335–350.
- DAVIS, T.L. & STERLING, P. (1979). Microcircuitry of cat visual cortex: Classification of neurons in layer IV of area 17, and identification of the pattern of lateral geniculate input. *Journal of Comparative Neurology* **188**, 599–627.
- DEBRUYN, E.J. & BONDS, A.B. (1986). Contrast adaptation in cat visual cortex is not mediated by GABA. *Brain Research* **383**, 339–342.
- DOUGLAS, R.J. & MARTIN, K.A.C. (1991). A functional microcircuit for cat visual cortex. *Journal of Physiology* **440**, 735–769.
- DOUGLAS, R.J., KOCH, C., MAHOWALD, M., MARTIN, K.A.C. & SUAREZ, H.H. (1995). Recurrent excitation in neocortical circuits. *Science* **269**, 981–985.
- DYKES, R.W., LANDRY, P., METHERATE, R. & HICKS, T.P. (1984). Functional role of GABA in cat primary somatosensory cortex: Shaping receptive fields of cortical neurons. *Journal of Neurophysiology* **52**, 1066–1093.
- EBNER, F.F. & COLONNIER, M. (1975). Synaptic patterns in the visual cortex of turtle: An electron microscopic study. *Journal of Comparative Neurology* **160**, 51–80.
- ECCLES, J. C. (1969). *The Inhibitory Pathways of the Central Nervous System*. Illinois: Charles C. Thomas Publishers.
- EYSEL, U.T. & SHEVELEV, I.A. (1994). Time-slice analysis of inhibition in cat striate cortical neurons. *Neuro Report* **5**, 2033–2036.

- FERSTER, D. & LINDSTRÖM, S. (1983). An intracellular analysis of geniculocortical connectivity in area 17 of the cat. *Journal of Physiology* (London) **342**, 181–215.
- FFRENCH-CONSTANT, R.H., ROCHELEAU, T.A., STEICHEN, J.C., & CHALMERS, A.E. (1993a). A point mutation in a *Drosophila* GABA receptor confers insecticide resistance. *Nature* **363**, 449–451.
- FFRENCH-CONSTANT, R.H., STEICHEN, J.C., ROCHELEAU, T.A., ARONSTEIN, K. & ROUSH, R.T. (1993b). A single amino acid substitution in a γ -aminobutyric acid subtype *a* receptor locus is associated with cyclodiene insecticide resistance in *Drosophila* populations. *Proceedings of the National Academy of Sciences of the U.S.A.* **90**, 1957–1961.
- FRANCESCETTI, S., GUATTEO, E., PANZICA, F., SANCINI, G., WANKE, E. & AVANZINI, G. (1995). Ionic mechanisms underlying burst firing in pyramidal neurons: Intracellular study in rat sensorimotor cortex. *Brain Research* **696**, 127–139.
- GALLAGHER, J.P., HIGASHI, H. & NISHI, S. (1978). Characterization and ionic basis of GABA-induced depolarizations recorded *in vitro* from cat primary afferent neurones. *Journal of Physiology* (London) **275**, 263–282.
- GAREY, L.J. & POWELL, T.P.S. (1971). An experimental study of the termination of the lateral geniculo-cortical pathway in the cat and monkey. *Proceedings of the Royal Society* (London) **179**, 41–63.
- GIL, Z. & AMITAL, Y. (1996). Properties of convergent thalamocortical and intracortical synaptic potentials in single neurons of neocortex. *Journal of Neuroscience* **16**, 6567–6578.
- GILBERT, C.D. (1983). Microcircuitry of the visual cortex. In *Annual Review of Neuroscience*, Vol. 6, ed. COWAN, W.M., SHOOTER, E.M., STEVENS, C.F. & THOMPSON, R.F., pp. 217–247. Palo Alto, California: Annual Reviews, Inc.
- GRANDA, A.M. & FULBROOK, J.E. (1989). Classification of turtle retinal ganglion cells. *Journal of Neurophysiology* **62**, 723–737.
- GRAY, C.M. & MCCORMICK, D.A. (1996). Chattering cells: Superficial pyramidal neurons contributing to the generation of synchronous oscillations in the visual cortex. *Science* **274**, 109–113.
- GUPTA, A., WANG, Y. & MARKRAM, H. (2000) Organizing principles for a diversity of GABAergic interneurons and synapses in the neocortex. *Science* **287**, 273–278.
- HICKS, T.P. & DYKES, R.W. (1983). Receptive field size for certain neurons in primary somatosensory cortex is determined by GABA-mediated intracortical inhibition. *Brain Research* **274**, 160–164.
- HWA, G.G.C. & AVOLI, M. (1992). Excitatory postsynaptic potentials recorded from regular-spiking cells in layers II/III of rat sensorimotor cortex. *Journal of Neurophysiology* **67**, 728–737.
- INOMATA, N., TOKUTOMI, N., OYAMA, Y. & AKAIKE, N. (1988). Intracellular picrotoxin blocks pentobarbital-gated Cl⁻ conductance. *Neuroscience Research* **6**, 72–75.
- INOUE, M. & AKAIKE, N. (1988). Blockade of γ -aminobutyric acid-gated chloride current in frog sensory neurons by picrotoxin. *Neuroscience Research* **5**, 380–394.
- KAWAGUCHI, Y. (1993). Groupings of nonpyramidal and pyramidal cells with specific physiological and morphological characteristics in rat frontal cortex. *Journal of Neurophysiology* **69**, 416–431.
- KAWAGUCHI, Y. (1995). Physiological subgroups of nonpyramidal cells with specific morphological characteristics in layer II/III of rat frontal cortex. *Journal of Neuroscience* **15**, 2638–2655.
- KAWAGUCHI, Y. & KUBOTA, Y. (1997). GABAergic cell subtypes and their synaptic connections in rat frontal cortex. *Cerebral Cortex* **7**, 476–486.
- KRIEGSTEIN, A.R. (1987). Synaptic responses of cortical pyramidal neurons to light stimulation in the isolated turtle visual system. *Journal of Neuroscience* **7**, 2488–2492.
- KRIEGSTEIN, A.R. & CONNORS, B.W. (1986). Cellular physiology of the turtle visual cortex: Synaptic properties and intrinsic circuitry. *Journal of Neuroscience* **6**, 178–191.
- KRNJEVIC, K., MITCHELL, J.F. & SZERB, J.C. (1963). Determination of iontophoretic release of acetylcholine from micropipettes. *Journal of Physiology* **165**, 421–436.
- KYRIAZI, H.T., CARVELL, G.E., BRUMBERG, J.C. & SIMON, D.J. (1996). Quantitative effects of GABA and bicuculline methiodide on receptive field properties of neurons in real and simulated whisker barrels. *Journal of Neurophysiology* **75**, 547–560.
- LARSON-PRIOR, L.J., ULINSKI, P.S. & SLATER, N.T. (1991). Excitatory amino acid receptor-mediated transmission in geniculocortical and intracortical pathways within visual cortex. *Journal of Neurophysiology* **66**, 293–306.
- LI, C.L. (1963). Cortical intracellular synaptic potentials in response to thalamic stimulation. *Journal of Cellular and Comparative Physiology* **61**, 165–179.
- LI, C.L., ORTIZ-GALVIN, A., CHOU, S.N. & HOWARD, S. (1960). Cortical intracellular potentials in response to stimulation of the lateral geniculate body. *Journal of Neurophysiology* **23**, 592–601.
- MACDONALD, R.L. & OLSEN, R.W. (1994). GABA_A receptor channels. *Annual Review of Neuroscience* **17**, 569–602.
- MAKSAY, G. & TICKU, M.K. (1985). Dissociation of [35S]t-butylbicyclophosphorothionate binding differentiates convulsant and depressant drugs that modulate GABAergic transmission. *Journal of Neurochemistry* **44**, 480–486.
- MANCILLA, J.G. & ULINSKI, P.S. (1995). Quantitative analysis of EPSPs in pyramidal cells of visual cortex. *Society for Neuroscience Abstracts* **21**, 596.
- MANCILLA, J.G., FOWLER, M. & ULINSKI, P.S. (1998). Responses of regular spiking and fast spiking cells in turtle visual cortex to light flashes. *Visual Neuroscience* **15**, 979–993.
- MARCHIAFAVA, P.L. (1983). An “antagonistic” surround facilitates central responses by retinal ganglion cells. *Vision Research* **23**, 1097–1099.
- MASUMI, I. & AKAIKE, N. (1988). Blockade of γ -aminobutyric acid-gated chloride current in frog sensory neurons by picrotoxin. *Neuroscience Research* **5**, 380–394.
- MCCORMICK, D.A., CONNORS, B.W., LIGHTHALL, J.W. & PRINCE, D.A. (1985). Comparative electrophysiology of pyramidal and sparsely spiny stellate neurons of the neocortex. *Journal of Neurophysiology* **54**, 782–806.
- METHERATE, R. & ASHE, J.H. (1993). Ionic flux contributions to neocortical slow waves and nucleus basalis-mediated activation: Whole-cell recordings *in vivo*. *Journal of Neuroscience* **13**, 5312–5323.
- METHERATE, R. & ASHE, J.H. (1994). Facilitation of an NMDA receptor-mediated EPSP by paired-pulse stimulation in rat neocortex *via* depression of GABAergic IPSPs. *Journal of Physiology* (London) **481**, 331–348.
- MORI, K., NOWYCKY, M.C. & SHEPHERD, G.M. (1981). Electrophysiological analysis of mitral cells in the isolated turtle olfactory bulb. *Journal of Physiology* (London) **314**, 281–294.
- NELSON, S. (1991). Temporal interactions in the cat visual system. III. Pharmacological studies of cortical suppression suggest a presynaptic mechanism. *Journal of Neuroscience* **11**, 369–380.
- NELSON, S., TOTH, L., SHETH, B. & SUR, M. (1994). Orientation selectivity of cortical neurons during intracellular blockade of inhibition. *Science* **265**, 774–777.
- NEWLAND, C.F. & CULL-CANDY, S.G. (1992). On the mechanism of action of picrotoxin on GABA receptor channels in dissociated sympathetic neurones of the rat. *Journal of Physiology* **447**, 191–213.
- PATEL, H.H. & SILLITO, A.M. (1978). Inhibition and velocity tuning in the cat visual cortex. *Journal of Physiology* **284**, 113p–114p.
- PETERS, A. & FELDMAN, M. (1976). The projection of the lateral geniculate nucleus to area 17 of the rat cerebral cortex. I. General description. *Journal of Neurocytology* **5**, 63–84.
- PETERS, A. & FAIRÉN, A. (1978). Smooth and sparsely-spined stellate cells in the visual cortex of the rat: A study using a combined Golgi-electron microscope technique. *Journal of Comparative Neurology* **181**, 129–172.
- PETERS, A., FELDMAN, M. & SALDANHA, J. (1976). The projection of the lateral geniculate nucleus to area 17 of the rat cerebral cortex. II. Terminations upon neuronal perikarya and dendritic shafts. *Journal of Neurocytology* **5**, 85–107.
- PIVOVAROV, A.S. & TREPANOV, V.V. (1972). Intracellular analysis of unit responses to afferent stimulation in the general and hippocampal cortex of turtles. *Neuroscience Behavior Physiology* **6**, 144–150.
- PURVES, R.D. (1981). *Microelectrode Methods for Intracellular Recording and Ionophoresis*, pp. 92–102. New York: Academic Press, Inc.
- SATO, H., KATSUYAMA, N., TAMURA, H., HATA, Y. & TSUMOTO, T. (1995). Mechanisms underlying direction selectivity of neurons in the primary visual cortex of the macaque. *Journal of Neurophysiology* **74**, 1382–1394.
- SATO, H., KATSUYAMA, N., TAMURA, H., HATA, Y. & TSUMOTO, T. (1996). Mechanisms underlying orientation selectivity of neurons in the primary visual cortex of the macaque. *Journal of Physiology* **494.3**, 757–771.
- SILLITO, A.M. (1975). The contribution of inhibitory mechanisms to the receptive field properties of neurones in the striate cortex of the cat. *Journal of Physiology* **250**, 305–329.
- SILLITO, A.M. (1977). Inhibitory processes underlying the directional specificity of simple, complex and hypercomplex cells in the cat's visual cortex. *Journal of Physiology* **271**, 699–720.

- SILLITO, A.M. (1979). Inhibitory mechanisms influencing complex cell orientation selectivity and their modification at high resting discharge levels. *Journal of Physiology* **289**, 33–53.
- SILLITO, A.M. & VERSIANI, V. (1976). Synaptic mechanisms contributing to the length preference of hypercomplex cells. *Journal of Physiology* **263**, 171p–172p.
- SILLITO, A.M., KEMP, J.A. & PATEL, H. (1980). Inhibitory interactions contributing to the ocular dominance of monocularly dominated cells in the normal cat striate cortex. *Experimental Brain Research* **41**, 1–10.
- SMART, T.G. & CONSTANTI, A. (1986). Studies on the mechanism of action of picrotoxin and other convulsants at the crustacean muscle GABA receptor. *Proceedings of the Royal Society (London)* **227**, 191–216.
- SMITH, L.M., EBNER, F.F. & COLONNIER, M. (1980). The thalamocortical projection in *Pseudemys* turtles: A quantitative electron microscope study. *Journal of Comparative Neurology* **190**, 445–462.
- SUAREZ, H., KOCH, C. & DOUGLAS, R. (1995). Modeling direction selectivity of simple cells in striate visual cortex within the framework of the canonical microcircuit. *Journal of Neuroscience* **15**, 6700–6719.
- THOMSON, A.M., WEST, D.C., HAHN, J. & DEUCHARS, J. (1996). Single axon IPSPs elicited in pyramidal cells by three classes of interneurons in slices of rat neocortex. *Journal of Physiology* **496**, 81–102.
- TSUMOTO, T., ECKART, W. & CREUTZFELDT, O.D. (1979). Modification of orientation sensitivity of cat visual cortex neurons by removal of GABA-mediated inhibition. *Experimental Brain Research* **34**, 351–363.
- VIDYASAGAR, T.R. & MUELLER, A. (1994). Function of GABA_A inhibition in specifying spatial frequency and orientation selectivities in cat striate cortex. *Experimental Brain Research* **98**, 31–38.
- WATANABE, S., KONISHI, M. & CREUTZFELDT, D. (1966). Postsynaptic potentials in the cat's visual cortex following electrical stimulation of afferent pathways. *Experimental Brain Research* **1**, 272–283.
- XU, M., COVEY, D.F. & AKABAS, M.H. (1995). Interaction of picrotoxin with GABA_A receptor channel-lining residues probed in cysteine mutants. *Biophysical Journal* **69**, 1858–1867.
- YAKUSHIJI, T., TOKUTOMI, N., AKAIKE, N. & CARPENTER, D.O. (1987). Antagonists of GABA responses, studied using internally perfused frog dorsal root ganglion neurons. *Neuroscience* **22**, 1123–1133.
- YOON, K., COVEY, D.F. & ROTHMAN, S.M. (1993). Multiple mechanisms of picrotoxin block of GABA-induced currents in rat hippocampal neurons. *Journal of Physiology* **464**, 423–439.